
Figures and figure supplements

Short and long sleeping mutants reveal links between sleep and macroautophagy

Joseph L Bedont et al

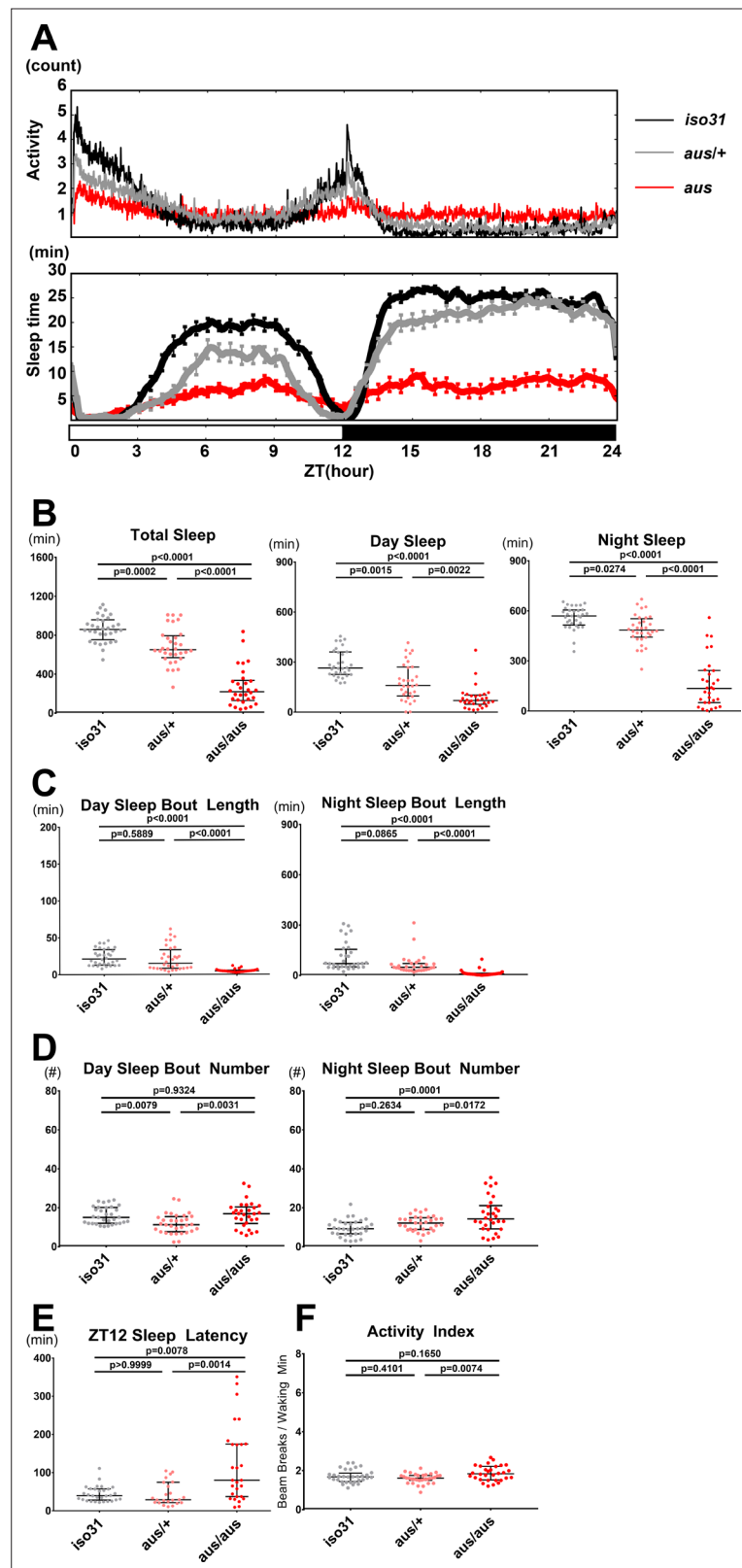


Figure 1. Sleep phenotype of *argus* mutants. All sleep metrics were measured under a 12 hr:12 hr light:dark cycle in female *iso31* (gray), *aus/+* (pink) and *aus/aus* (red) flies. **(A)** Mean activity (top panel) and sleep (bottom panel) over time during the 24-hr cycle. **(B)** Total sleep amount during the whole 24-hr cycle (left), day (middle), and night (right). **(C)** Mean sleep bout duration during the day (left) and night (right). **(D)** Sleep bout number

Figure 1 continued on next page

Figure 1 continued

during the day (left) and night (right). **(E)** Latency to first sleep bout after ZT12 lights off. **(F)** Activity index of beam breaks per waking minute over the 24-hr cycle. $n = 30\text{--}32$ (**A–D,F**) or $n = 23\text{--}30$ (**E**); individual flies overlaid with median \pm interquartiles (**B–F**); Tukey test (B-total+ night,C,F) or Dunn test (B-day,D-E). **(A)**.

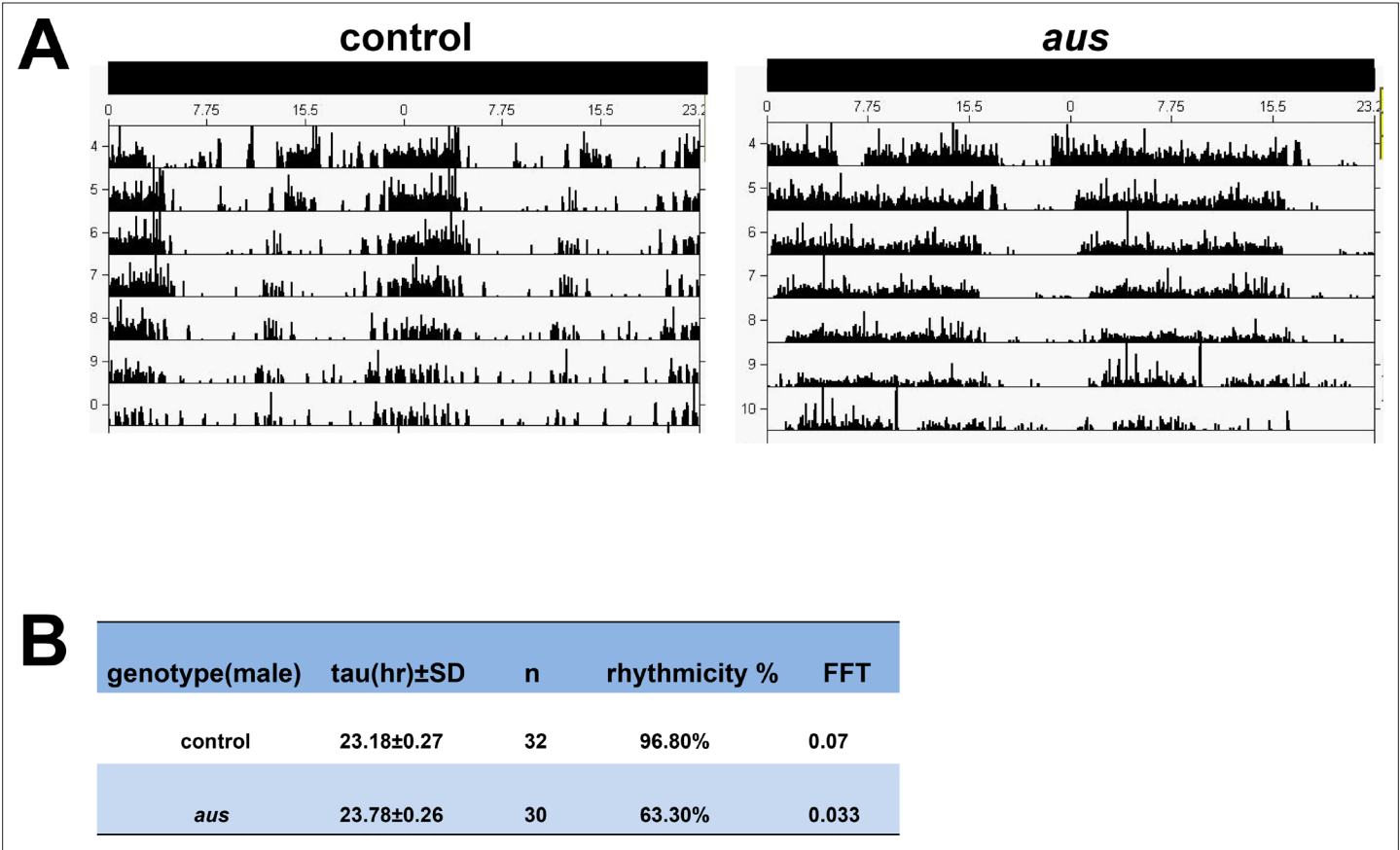


Figure 1—figure supplement 1. Circadian rhythms are intact in the *aus* mutant. **(A)** Sample actograms from *iso31* control and *aus* mutant flies. **(B)** Activity data from flies assayed during constant darkness were assessed for circadian rhythmicity. Average circadian period length (τ) of *iso31* controls and *aus* mutants was based on Clocklab analysis. Fast Fourier Transform (FFT) was used to establish a cutoff for rhythmicity, such that FFT values > 0.01 were considered indicative of a rhythm. The average FFT value is calculated from rhythmic flies.

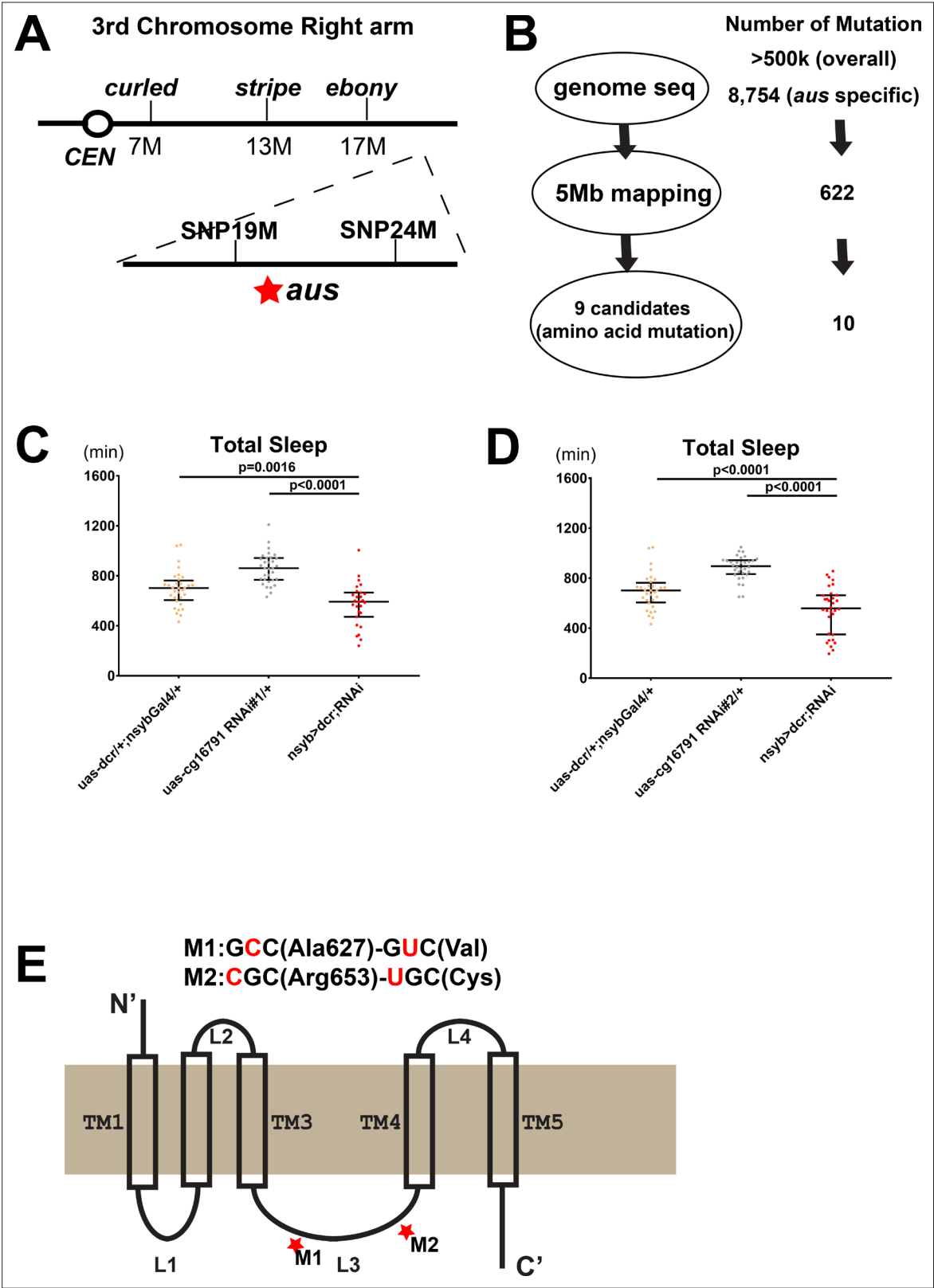


Figure 2. Mapping the *argus* sleep phenotype to a single gene: *cg16791*. (A) The genomic location of *argus* is indicated as a star within a 5 Mb region on the right arm of the third chromosome, following genetic mapping with visible mutations and SNP markers. (B) Schematic of the genome sequencing procedure of *argus* homozygotes with the number of mutations identified in each step listed on the right. The initial alignment revealed more than half a million mutations relative to the published *Drosophila* genome. More than eight thousand mutations remained after removing mutations also found in other *Drosophila* species. (C) Scatter plot of total sleep time (min) for *uas-dcr1+;nsybGal4/+*, *uas-cg16791 RNAi#1/+*, and *nsyb>dcr;RNAi* genotypes. (D) Scatter plot of total sleep time (min) for *uas-dcr1+;nsybGal4/+*, *uas-cg16791 RNAi#2/+*, and *nsyb>dcr;RNAi* genotypes. (E) Schematic diagram of the protein structure showing transmembrane domains (TM1-TM5) and loops (L1-L4). Mutations M1 and M2 are indicated by red stars in loops L3 and L4 respectively.

Figure 2 continued on next page

Figure 2 continued

in the *iso31* control strain. Factoring in the mapping data (shown in A) and focusing on missense mutations narrowed the number of candidate genes to nine. **(C–D)** Total sleep with *cg16791* RNAi knockdown in females, using pan-neuronal driver *nsyb-Gal4*, *uas-dicer*, and either of two independent RNAi lines, compared to RNAi-alone and *nsyb-Gal4+ Dcr* alone controls. $n = 27\text{--}32$; Fischer's LSD; individual flies overlaid with median \pm interquartiles. **(E)** Predicted protein of CG16791. Two GC-AT transitions that cause missense mutations in the loop3 region were identified by Sanger-sequencing in *aus* mutants.

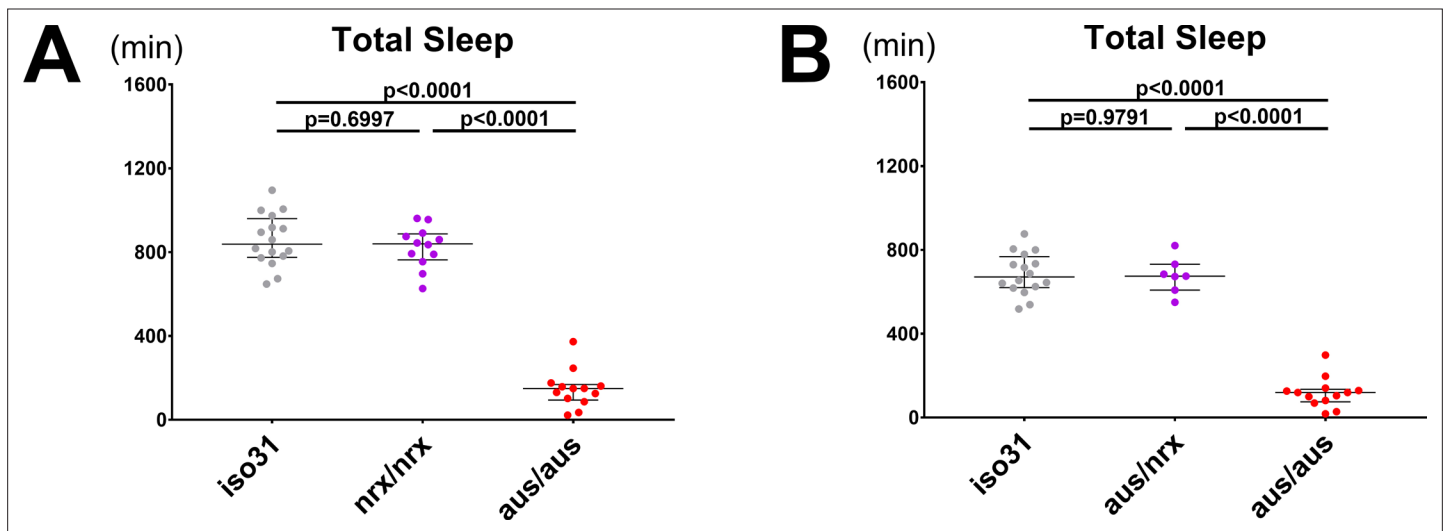
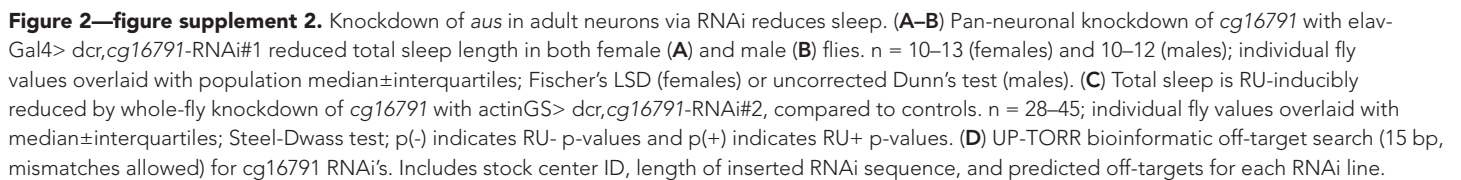


Figure 2—figure supplement 1. A mutation in *Nrx1* does not underlie the *aus* reduced sleep phenotype. **(A)** Total sleep in *nrx/nrx* mutants is comparable to iso31 control and greater than *aus/aus* mutants. $n = 12-16$; individual brain values overlaid with population median \pm interquartiles; Tukey test. **(B)** Total sleep in *Nrx/aus* transheterozygotes is comparable to iso31 control and greater than *aus/aus* mutants. $n = 7-16$; individual brain values overlaid with population median \pm interquartiles; Tukey test.



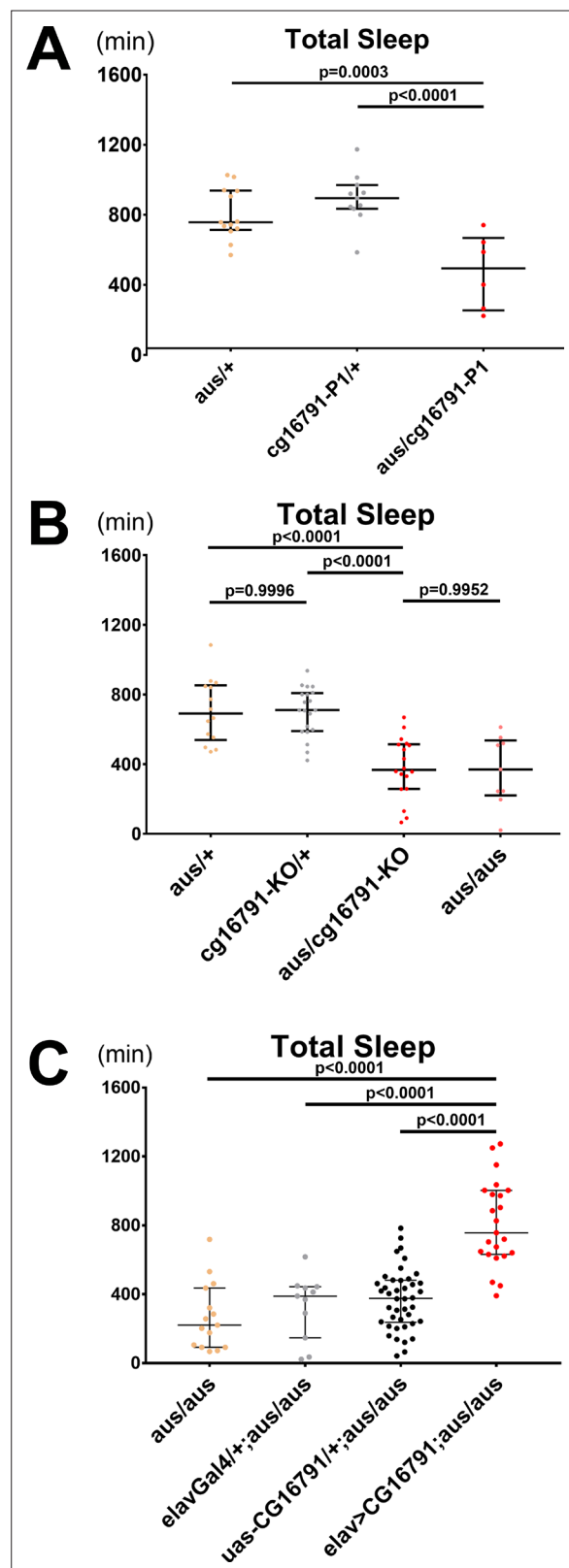


Figure 3. CG16791 underlies the *argus* sleep phenotype. **(A)** Transheterozygotes of male *aus* and *cg16791* insertional mutant (P1) have reduced total sleep compared to *aus/+* and *cg16791-P1/+* controls. $n = 6-13$; individual flies overlaid with median \pm interquartiles; Fischer's LSD. **(B)** Female *cg16791-KO* and *aus* (EMS) transheterozygotes have reduced total sleep compared to *aus* (EMS) or *cg16791-KO* heterozygotes.

Figure 3 continued on next page

Figure 3 continued

Transheterozygote total sleep is comparable to *aus* homozygotes. $n = 9\text{--}20$; individual flies overlaid with median \pm interquartiles; Tukey test. **(C)** Pan-neuronal expression of *uas-cg16791* with *elav-Gal4* partially rescues female *aus* homozygote short-sleep, to significantly above *aus*-homozygous *Gal4* and *UAS* controls. $n = 11\text{--}42$; individual flies overlaid with median \pm interquartiles; Fischer's LSD.

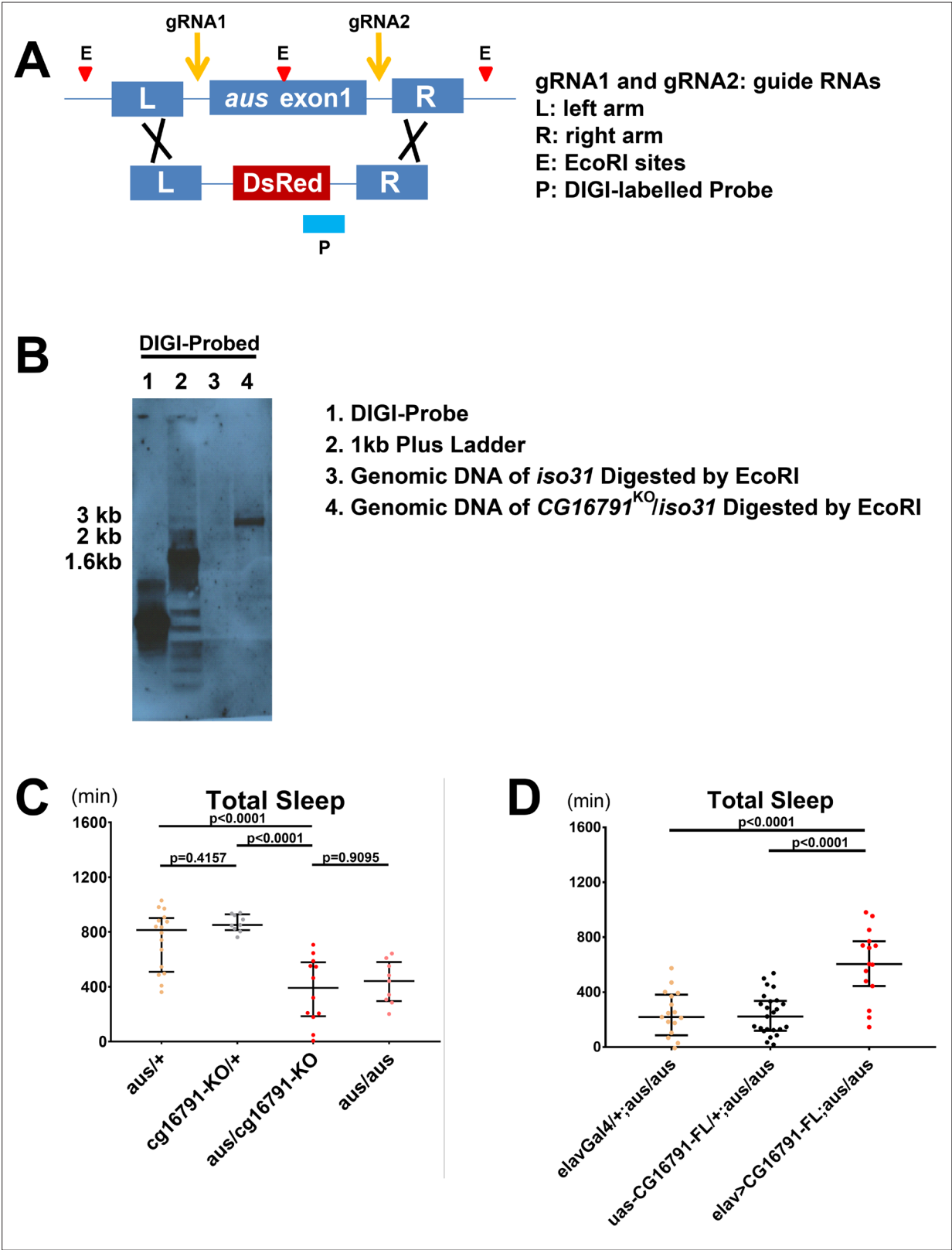


Figure 3—figure supplement 1. CRISPR-targeting of *argus* to generate a null mutant; supplemental Crispr-KO and full-length rescue data. **(A)** CRISPR-targeting of *argus* exon1 to replace it with a selectable marker, *Dsred*. **(B)** Southern blot analysis of *CG16791* (KO) using part of the *Dsred* gene as DIGI-probe. A single ~3 kb DIGI-positive band is expected for correct integration of *Dsred* at the *argus* locus. A small amount of DIGI label (< 1 ng) was loaded in lane1 as a control. The Life Science 1 kb plus ladder was loaded in lane 2, and non-specific binding with DIGI probe was observed. *iso31*

Figure 3—figure supplement 1 continued on next page

Figure 3—figure supplement 1 continued

gDNA digested by EcoRI in lane three or CG16791 KO/iso31 gDNA digested by EcoRI in lane 4. **(C)** Male *cg16791*-KO and *aus* (EMS) transheterozygotes have reduced total sleep compared to *aus* (EMS) or *cg16791*-KO heterozygotes. Transheterozygote total sleep is comparable to *aus* homozygotes. $n = 9$ – 16 ; individual flies overlaid with median \pm interquartiles; Tukey test. **(D)** Pan-neuronal expression of *uas-cg16791*(full-length) with *elav*-Gal4 partially rescues female *aus* homozygote short-sleep, to significantly above *aus*-homozygous Gal4 and UAS controls. $n = 15$ – 25 ; individual flies overlaid with median \pm interquartiles; Fischer's LSD.

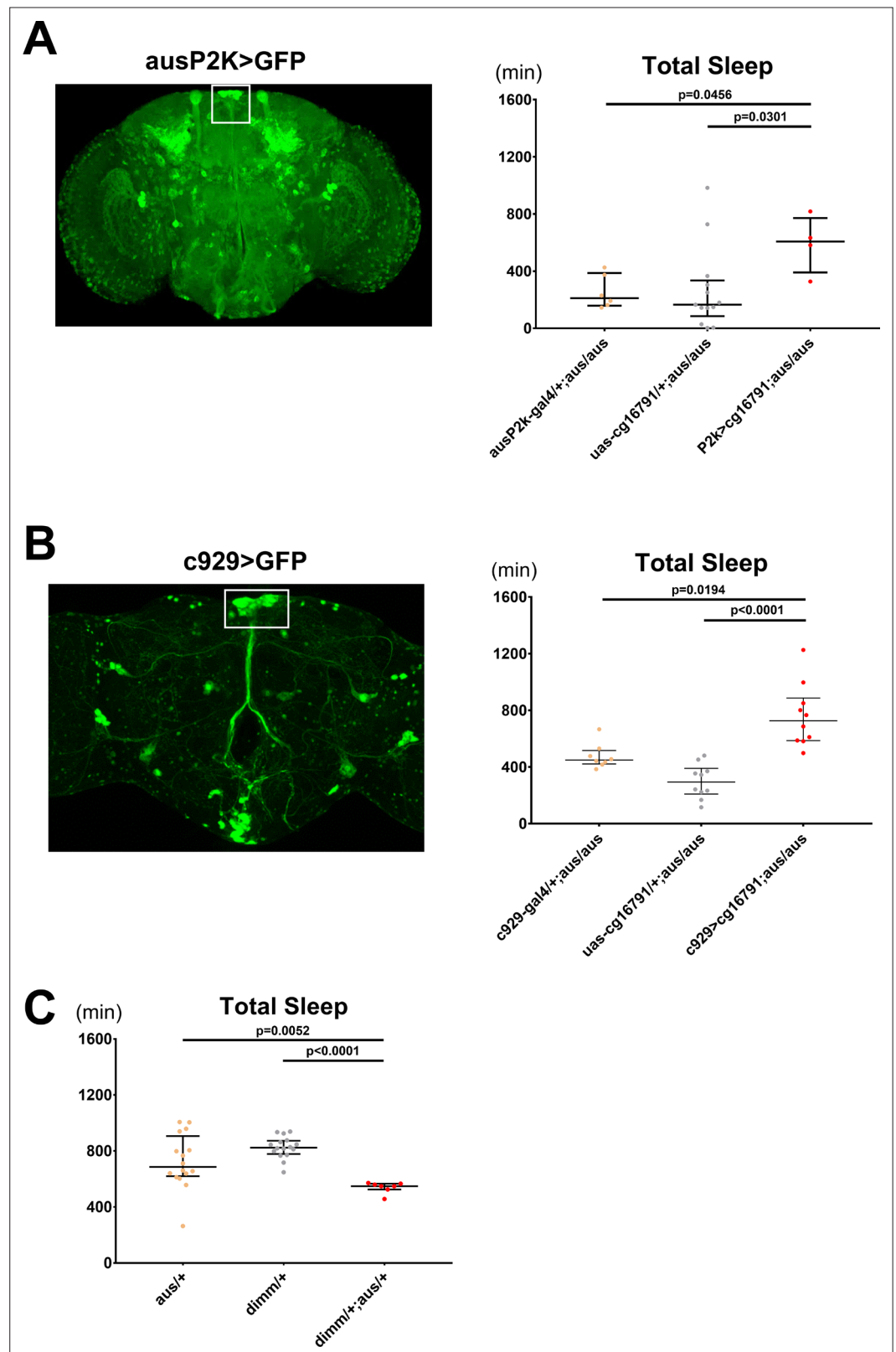


Figure 4. Argus functions in dimmed positive neurons to regulate sleep. **(A)** The *aus* promoter region was subcloned, and a ~ 2000 bp sequence was inserted upstream of Gal4 and used to drive GFP (left). *aus2kGal4* driving *uas-cg16791* partially rescues the short sleep phenotype in female fruit flies (*ausP2K*, UAS-*cg16791*, or *ausP2K* > UAS-*cg16791* in *aus/aus* mutant background). *n* = 4–13; individual flies overlaid with

Figure 4 continued on next page

Figure 4 continued

median±interquartiles; Fischer's LSD. **(B)** C929-Gal4 (a peptidergic Gal4 line representing Dimmed expression) driving GFP (left). C929 driving *uas-cg16791* expression rescues the short sleep phenotype in male *aus* flies. (*c929*, *UAS-cg16791*, or *c929> UAS-cg16791* in *aus/aus* mutant background). *n* = 8–10; individual flies overlaid with median±interquartiles; uncorrected Dunn's test. **(C)** *aus* and *dimm* interact genetically in female transheterozygotes to reduce sleep (*aus/+*, *dimm/+*, and *aus dim* transheterozygotes). *n* = 7–16; individual flies overlaid with median±interquartiles; uncorrected Dunn's test.

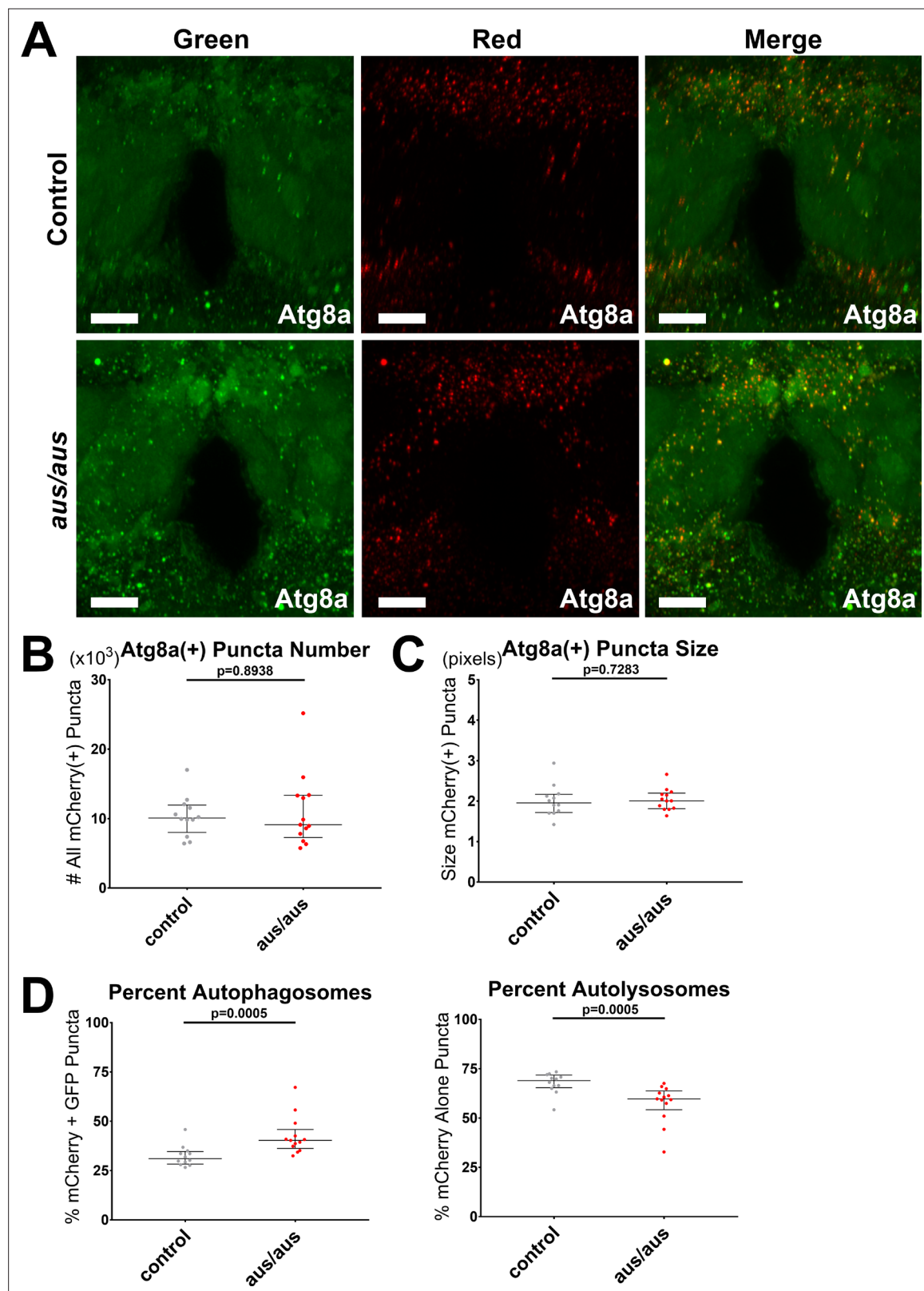


Figure 5. The *argus* mutant displays accumulation of autophagosomes. Female *iso31* control and *aus/aus* brains with *elav-Gal4* > *UAS-GFP-mCherry-Atg8a* driving pan-neuronal autophagy sensor were live imaged from ZT0-2. mCherry fluoresces in all Atg8a(+) puncta, while GFP fluoresces in autophagosomes and is quenched in autolysosomes. **(A)** Max-projected z-stacks of representative brains showing GFP (left), mCherry (middle), and merged (right) fluorescence. Scale bar = 25 μ m. **(B)** The number of all neuronal mCherry(+) puncta was similar in both genotypes. **(C)** The size of

Figure 5 continued on next page

Figure 5 continued

all neuronal mCherry(+) puncta was similar in both genotypes. **(D)** *aus* neuronal mCherry(+) puncta were significantly skewed toward % mCherry+ GFP(+) autophagosomes (left) and away from % mCherry-only(+) autolysosomes (right) compared to control. n = 12–13; individual brains overlaid with median±interquartiles; Mann-Whitney tests.

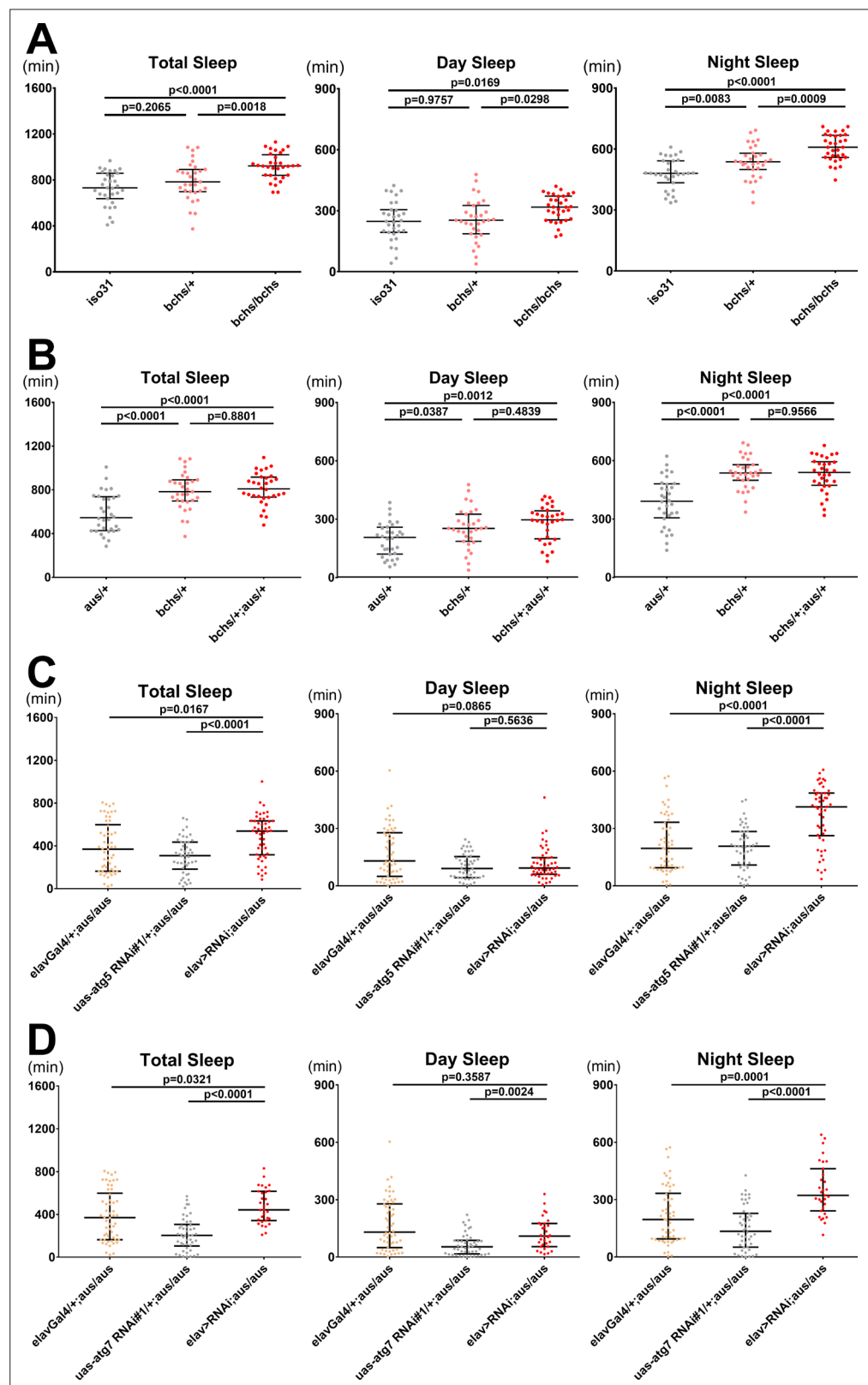


Figure 6. Blocking autophagosome production rescues the short sleep phenotype of the *argus* mutant. (A) Total, day, and night sleep were measured under 12 hr:12 hr light:dark in *iso31* control, *bchs/+*, and *bchs/bchs* female flies. $n = 31$ –32; individual flies overlaid with median \pm interquartiles; Tukey tests. (B) Total, day, and night sleep were measured under 12 hr:12 hr light:dark in *aus/+*, *bchs/+*, and *bchs/+; aus/+* transheterozygous female flies.

Figure 6 continued on next page

Figure 6 continued

n = 31–32; individual flies overlaid with median±interquartiles; Tukey tests. **(C–D)** Total, day, and night sleep were measured under 12 hr:12 hr light:dark in elav-Gal4/+ , UAS-RNAi/+ and elav-Gal4> UAS RNAi female flies in *aus/aus* mutant background. RNAi's used were atg5 RNAi#1 **(C)** and atg7 RNAi#1 **(D)**. n = 46–54 **(C)** or n = 31–54 **(D)**; individual flies overlaid with median±interquartiles; uncorrected Dunn's tests.

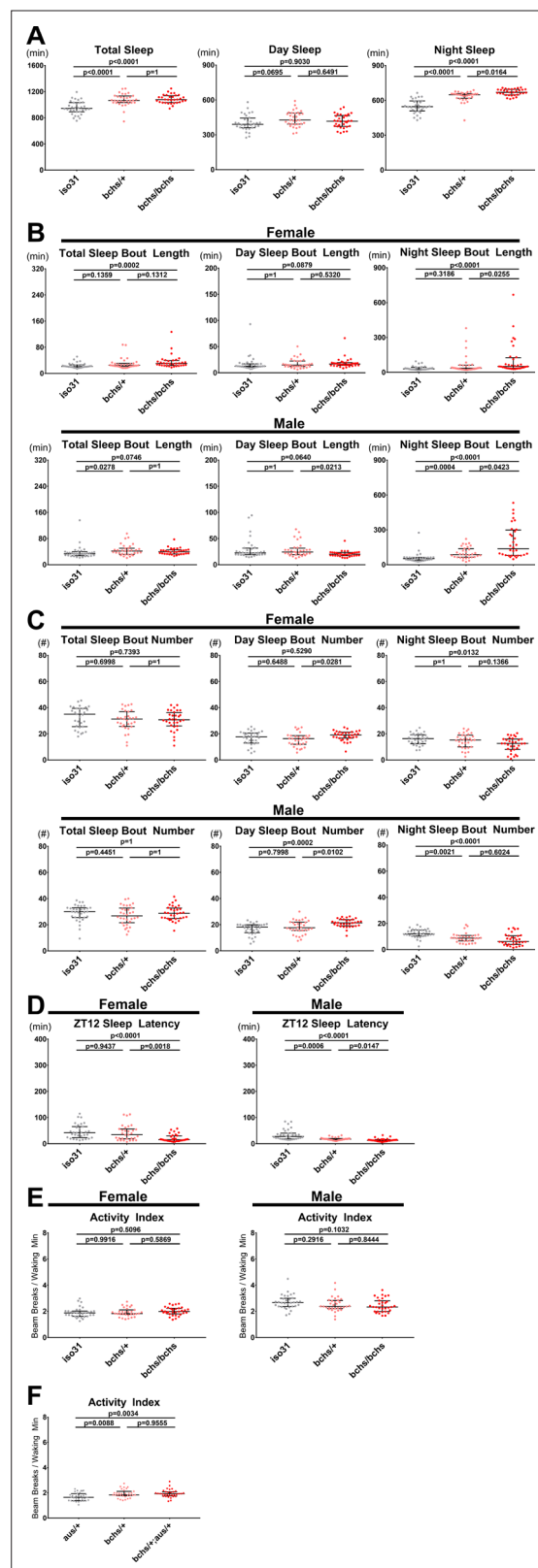


Figure 6—figure supplement 1. Effects of *aus* and *bchs* on sleep consolidation, latency, and activity index. (A–E) All sleep metrics were measured under a 12 hr:12 hr light:dark cycle in *iso31* (gray), *bchs/+* (pink) or *bchs/bchs* (red) flies. (A) Male total sleep amount during the whole 24-hr cycle (left), day (middle), and night (right). (B) Female (top) and male (bottom) mean sleep bout duration during the whole 24-hr cycle (left), day (middle) and night (right).

Figure 6—figure supplement 1 continued on next page

Figure 6—figure supplement 1 continued

(C) Female (top) and male (bottom) sleep bout number during the whole 24-hr cycle (left), day (middle) and night (right). (D) Female (left) and male (right) latency to first sleep bout after ZT12 lights off. (E) Female (left) and male (right) activity index of beam breaks per waking minute over the 24-hr cycle. (F) Activity index of beam breaks per waking minute over the 24-hr cycle in female *aus/+* (gray), *bchs/+* (pink) and transheterozygote (red) flies. *n* = 31–32; individual flies overlaid with median±interquartiles; Dunn tests (A–E) or Tukey test (F).

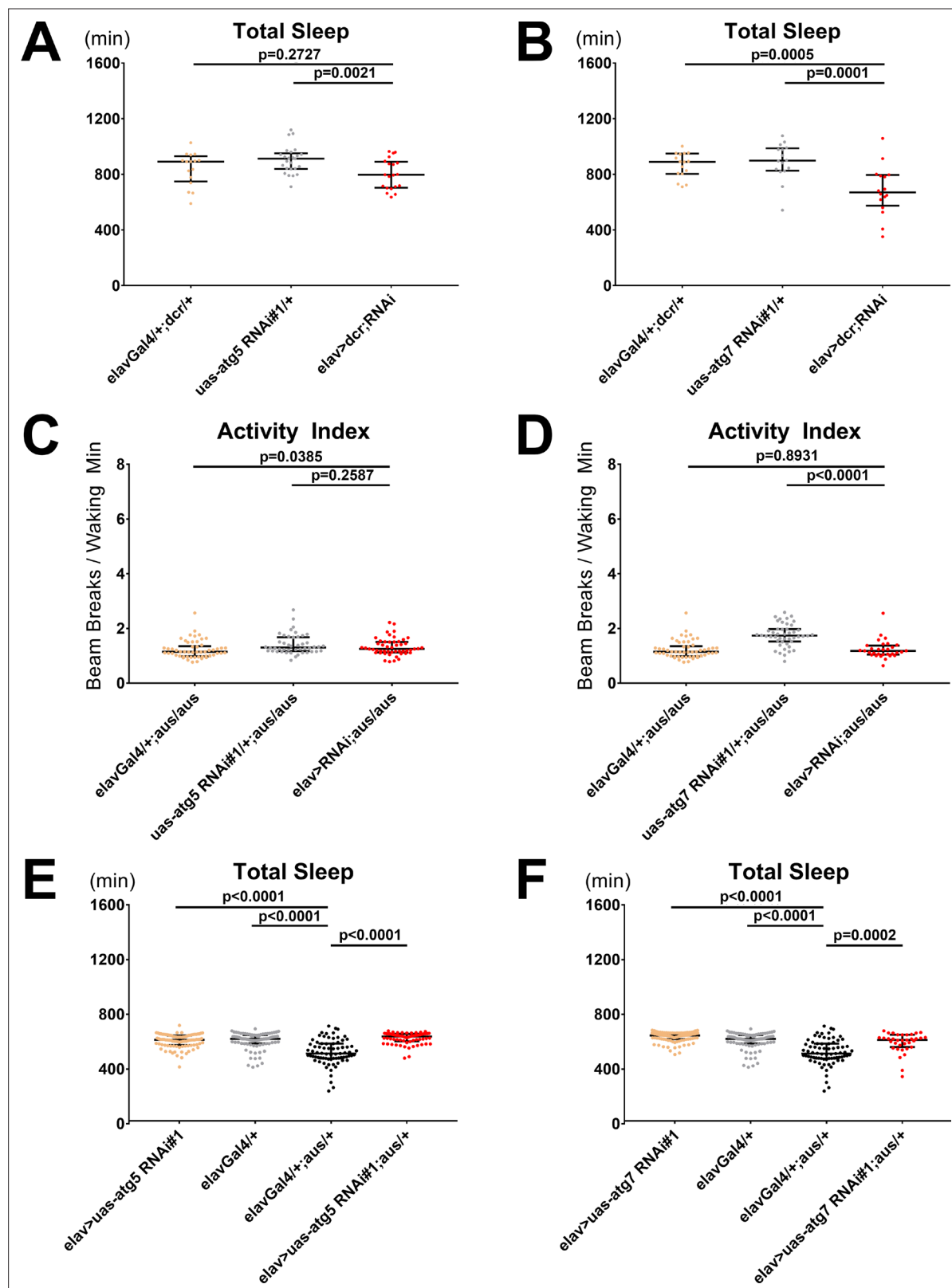


Figure 6—figure supplement 2. Rescue of *aus* mutants by *atg5/atg7* RNAi. (A–B) Total sleep amount with pan-neuronal *atg5* (A) or *atg7* (B) knockdown in female flies. *elav*⁺ *Dicer2*⁺, *UAS-atg* RNAi/+ or *elav*⁺ *Dicer2*[>] *UAS atg* RNAi. *n* = 16–25 (*atg5*) or *n* = 16 (*atg7*); individual flies overlaid with median±interquartiles; Fischer's LSD. (C–D) Activity index of beam breaks per waking minute over the 24-hr cycle in female *elav-Gal4*⁺, *UAS-atg* RNAi/+ or *elav-Gal4*/*UAS-atg* RNAi on *aus/aus* background. *atg5* RNAi (C) or *atg7* RNAi (D). *n* = 46–54 (C) or *n* = 31–54 (D); individual flies overlaid with

Figure 6—figure supplement 2 continued on next page

Figure 6—figure supplement 2 continued

median \pm interquartiles; uncorrected Dunn's test. (**E–F**) Total sleep amount in female *elav-Gal4/UAS-atg* RNAi, *elav-Gal4/+*, *elav-Gal4/+; aus/+* or *elav-Gal4/UAS-atg* RNAi, *aus/+*. *atg5* RNAi (**E**) or *atg7* RNAi (**F**). *n* = 65–92 (**E**) or *n* = 35–95; individual flies overlaid with median \pm interquartiles; uncorrected Dunn's test.

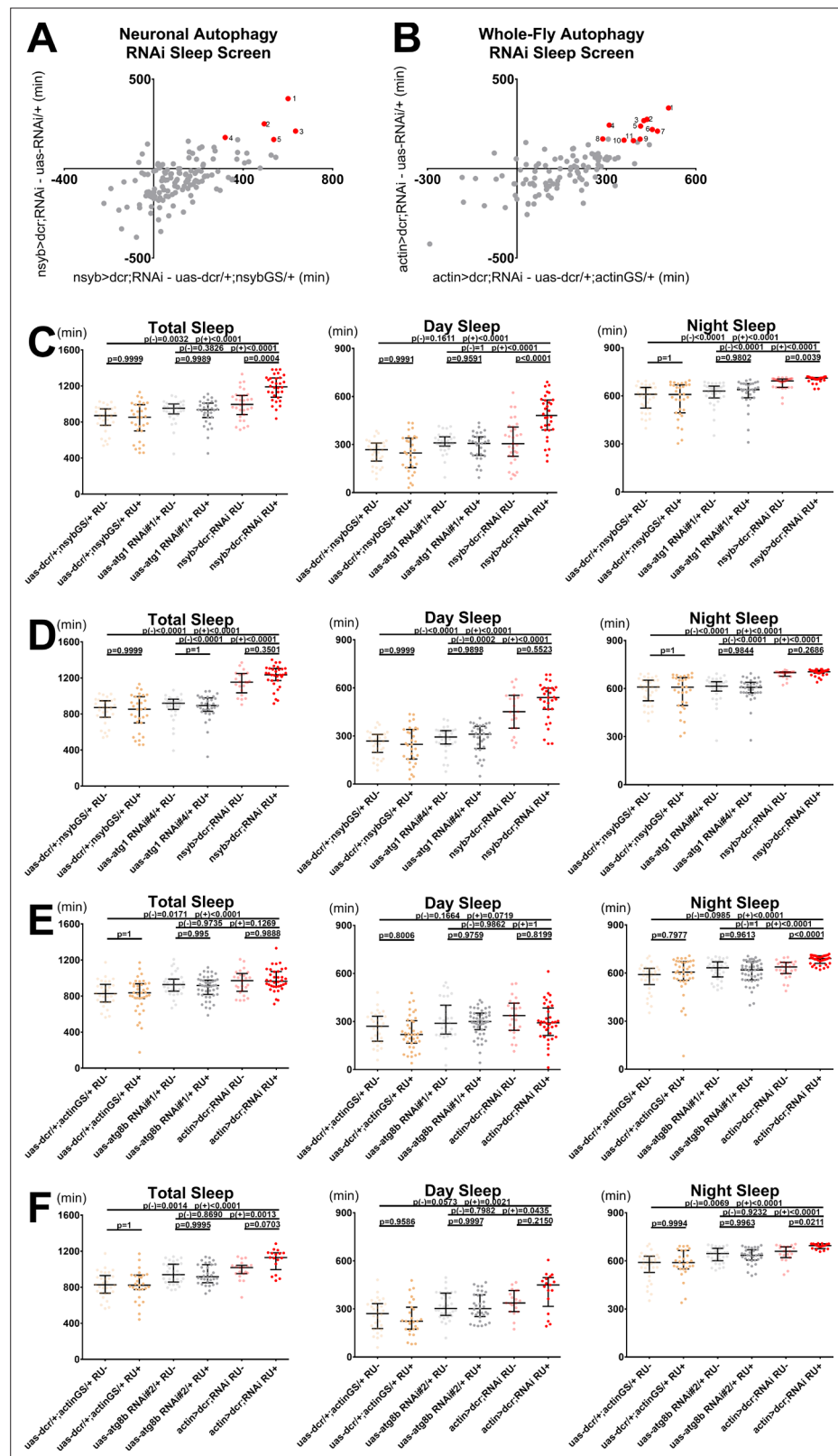


Figure 7. Blocking neuronal or whole-fly autophagosome formation increases sleep. **(A)** Difference in first-pass population median sleep on RU+ food for a range of female *nsybGS> dcr*;autophagy-RNAi crosses compared with *nsybGS> dcr* control (x-axis) and RNAi control (y-axis). Red, numbered dots indicate significant hits that passed all validation steps: (1) *bip* RNAi#3; (2) *atg1* RNAi#4; (3) *daor* RNAi#1; (4) *atg1* RNAi#1; (5) *atg10* RNAi#3. N = 133

Figure 7 continued on next page

Figure 7 continued

viable crosses shown; $n = 3\text{--}16$ flies per group for each first-pass experiment. **(B)** Difference in first-pass population median sleep on RU+ food for a range of female *actinGS> dcr;autophagy-RNAi* crosses compared with *actinGS> dcr* control (x-axis) and RNAi control (y-axis). Red, numbered dots indicate significant hits that passed all validation steps: (1) *dor* RNAi#2; (2) *atf6* RNAi#1; (3) *atg8b* RNAi#2; (4) *wacky* RNAi#2; (5) *atg8b* RNAi#1; (6) *atg7* RNAi#1; (7) *daor* RNAi#1; (8) *atg14* RNAi#3; (9) *dram* RNAi#2; (10) *aduk* RNAi#3; (11) *atg12* RNAi#2. $N = 106$ viable crosses shown; $n = 3\text{--}16$ flies per group for each first-pass experiment. See Supplementary file 3 for details on first-pass screen and **Figure 7—figure supplement 1** for combined first/second pass sleep data for significant hits, for the screens shown in both 7A and 7B. **(C–F)** Total (left), day (middle), and night (right) sleep in *GS> dcr;RNAi*, *GS> dcr* control, and RNAi control female flies on both RU+ and RU- food. All data shown as individual flies overlaid with median \pm interquartiles; p(-) indicates RU- p-values and p(+) indicates RU+ p-values. **(C)** *nsybGS> dcr;atg1-RNAi#1*: $n = 31\text{--}32$; Steel-Dwass test (total,night) and Tukey test. (day). **(D)** *nsybGS> dcr;atg1-RNAi#4*: $n = 21\text{--}32$; Steel-Dwass tests. **(E)** *actinGS> dcr;atg8b-RNAi#1*: $n = 25\text{--}47$; Steel-Dwass test (total,night) and Tukey test. (day). **(F)** *actinGS> dcr;atg8b-RNAi#2*: $n = 17\text{--}32$; Steel-Dwass tests.

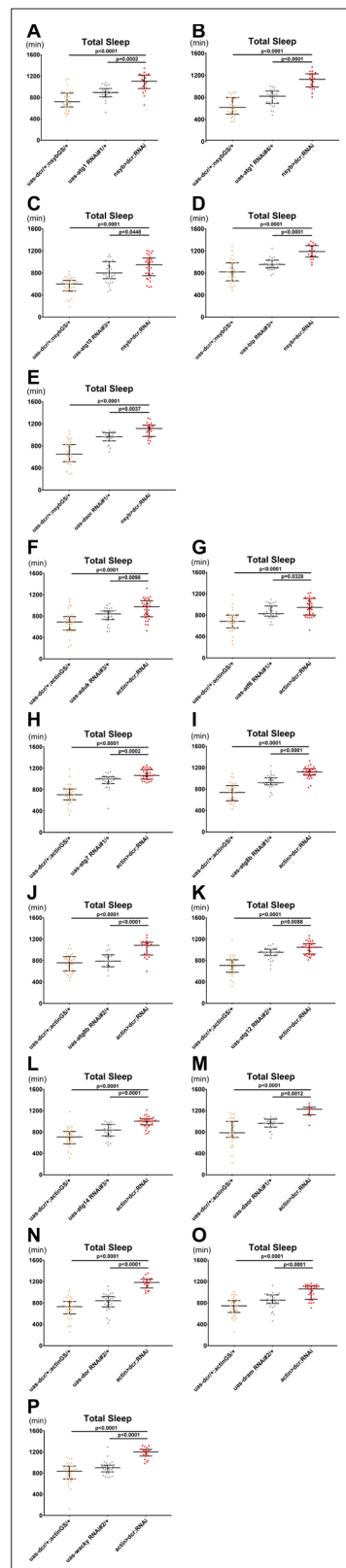


Figure 7—figure supplement 1. Validated hits from autophagy RNAi screens. (A–E) Total sleep amount in female UAS-dcr/+;nsybGS/+, UAS-RNAi/+;nsybGS>dcr,RNAi flies on RU+ food. (F–P) Total sleep amount

Figure 7—figure supplement 1 continued on next page

Figure 7—figure supplement 1 continued

in female UAS-dcr/+;actinGS/+, UAS-RNAi/+, or actinGS> dcr,RNAi flies on RU+ food. All data shown is individual flies overlaid with median±interquartiles. **(A)** nsybGS> dcr;atg1-RNAi#1: n = 20–31; Student's t-tests. **(B)** nsybGS> dcr;atg1-RNAi#4: n = 21–32; Student's t-tests. **(C)** nsybGS> dcr;atg10-RNAi#3: n = 30–32; Student's t-tests. **(D)** nsybGS> dcr;bip-RNAi#3: n = 18–31; Student's t-tests. **(E)** nsybGS> dcr;daor-RNAi#1: n = 22–31; Student's t-tests. **(F)** actinGS> dcr;aduk-RNAi#3: n = 31–32; Student's t-tests. **(G)** actinGS> dcr;atf6-RNAi#1: n = 30–32; Student's t-tests. **(H)** actinGS> dcr;atg7-RNAi#1: n = 31; Mann-Whitney tests. **(I)** actinGS> dcr;atg8b-RNAi#1: n = 29–31; Student's t-tests. **(J)** actinGS> dcr;atg8b-RNAi#2: n = 20–32; Student's t-tests. **(K)** actinGS> dcr;atg12-RNAi#2: n = 28–31; Student's t-tests. **(L)** actinGS> dcr;atg14-RNAi#3: n = 28–32; Student's t-tests. **(M)** actinGS> dcr;daor-RNAi#1: n = 9–31; Student's t-tests. **(N)** actinGS> dcr;dor-RNAi#2: n = 19–31; Student's t-tests. **(O)** actinGS> dcr;dram-RNAi#2: n = 30–31; Mann-Whitney tests. **(P)** actinGS> dcr;wacky-RNAi#2: n = 20–32; Mann-Whitney tests.

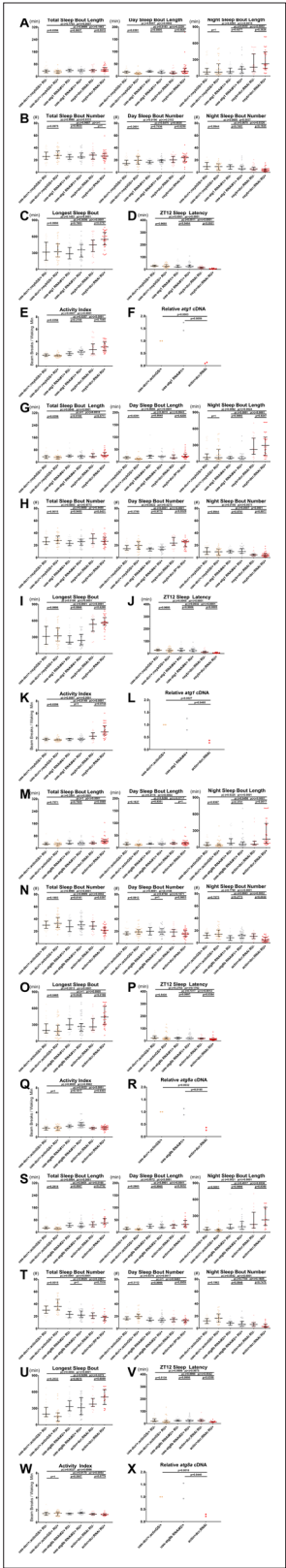


Figure 7—figure supplement 2. *atg1* and *atg8b* RNAi additional sleep metrics, activity index, and validation of knockdown. Additional metrics comparing GS+ UAS dcr control, UAS-RNAi control, and GS> dcr, RNAi

Figure 7—figure supplement 2 continued on next page

Figure 7—figure supplement 2 continued

females back-crossed to iso31, on both RU+ and RU- food. All data shown as individual flies overlaid with median±interquartiles (**A–E, G–K, M–Q, S–W**) or individual biological replicates (**F, L, R, X**); p(-) indicates RU- p-values and p(+) indicates RU+ p-values. (**A–F**) atg1-RNAi#1: experiments with nsybGS; n = 31–32 (**A–E**) or actinGS; n = 2 (**F**). (**G–L**) atg1-RNAi#4: experiments with nsybGS; n = 21–32 (**G–K**) or actinGS; n = 2 (**L**). (**M–R**) atg8b-RNAi#1: experiments with actinGS; n = 25–47 (**M–Q**) or actinGS; n = 2 (**R**). (**S–X**) atg8b-RNAi#2: experiments with actinGS; n = 17–32 (**S–W**) or actinGS; n = 2 (**X**). (**A, G, M, S**) Mean sleep bout duration during the whole 24-hr cycle (left), day (middle) and night (right). All comparisons are Steel-Dwass tests. (**B, H, N, T**) Sleep bout number during the whole 24-hr cycle (left), day (middle) and night (right). Comparisons are Tukey test (atg1 RNAi#1 day-bouts) or Steel-Dwass tests (all other comparisons). (**C, I, O, U**) Longest sleep bout during the whole 24-hr cycle. Comparisons are Tukey test (atg1 RNAi#1) or Steel-Dwass tests (all other comparisons). (**D, J, P, V**) Latency to first sleep bout after ZT12 lights off. All comparisons are Steel-Dwass tests. (**E, K, Q, W**) Activity index of beam breaks per waking minute over the 24-hr cycle. All comparisons are Steel-Dwass tests. (**F, L, R, X**) Relative cDNA expression level in whole-fly lysate. All comparisons are one-tailed t-tests.

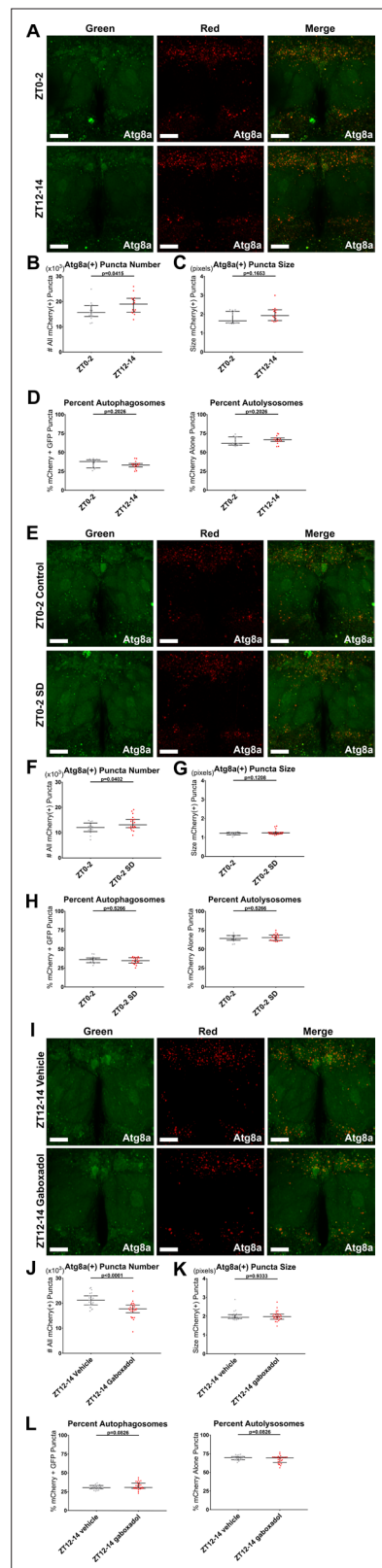


Figure 8. Sleep regulates autophagosome production. *elav-Gal4> UAS-GFP-mCherry-Atg8a* flies expressing pan-neuronal autophagy sensor were live imaged as follows. All quantification shows individual brain values

Figure 8 continued on next page

Figure 8 continued

overlaid with population median \pm interquartiles. **(A–D)** ZT0-2 or ZT12-14. $n = 15$; Student's t-tests. **(E–H)** ZT0-2 after either a control night of unchallenged sleep or at least 12 hr of mechanical sleep deprivation (SD) beginning at the prior ZT12. $n = 13–20$; Student's t-tests. **(I–L)** ZT12-14 after either a control day of feeding with vehicle or at least 11 hr of feeding with 0.1 mg/mL gaboxadol that verifiably and markedly increased daytime sleep, beginning at the prior ZT0-1. $n = 25–26$. **(A,E,I)** Max-projected z-stacks of representative brains showing GFP (left), mCherry (middle), and merged (right) fluorescence for ZT time comparison **(A)**, control vs SD **(E)**, or vehicle vs gaboxadol **(I)**. Scale bars = 25 μ m. **(B,F,J)** The number of all neuronal mCherry(+) puncta was higher at nightfall than daybreak **(B)**, elevated at daybreak by 12 hr overnight SD **(F)**, and depressed at nightfall by 12 hr daytime of gaboxadol-induced sleep **(J)**. **(C,G,K)** The size of all neuronal mCherry(+) puncta was unaffected by ZT time, SD, and gaboxadol. **(D,H,L)** The percentage of neuronal mCherry(+) puncta that are mCherry+GFP(+) autophagosomes (left) and mCherry-only(+) autolysosomes (right) was unaffected by ZT time, SD, and gaboxadol.

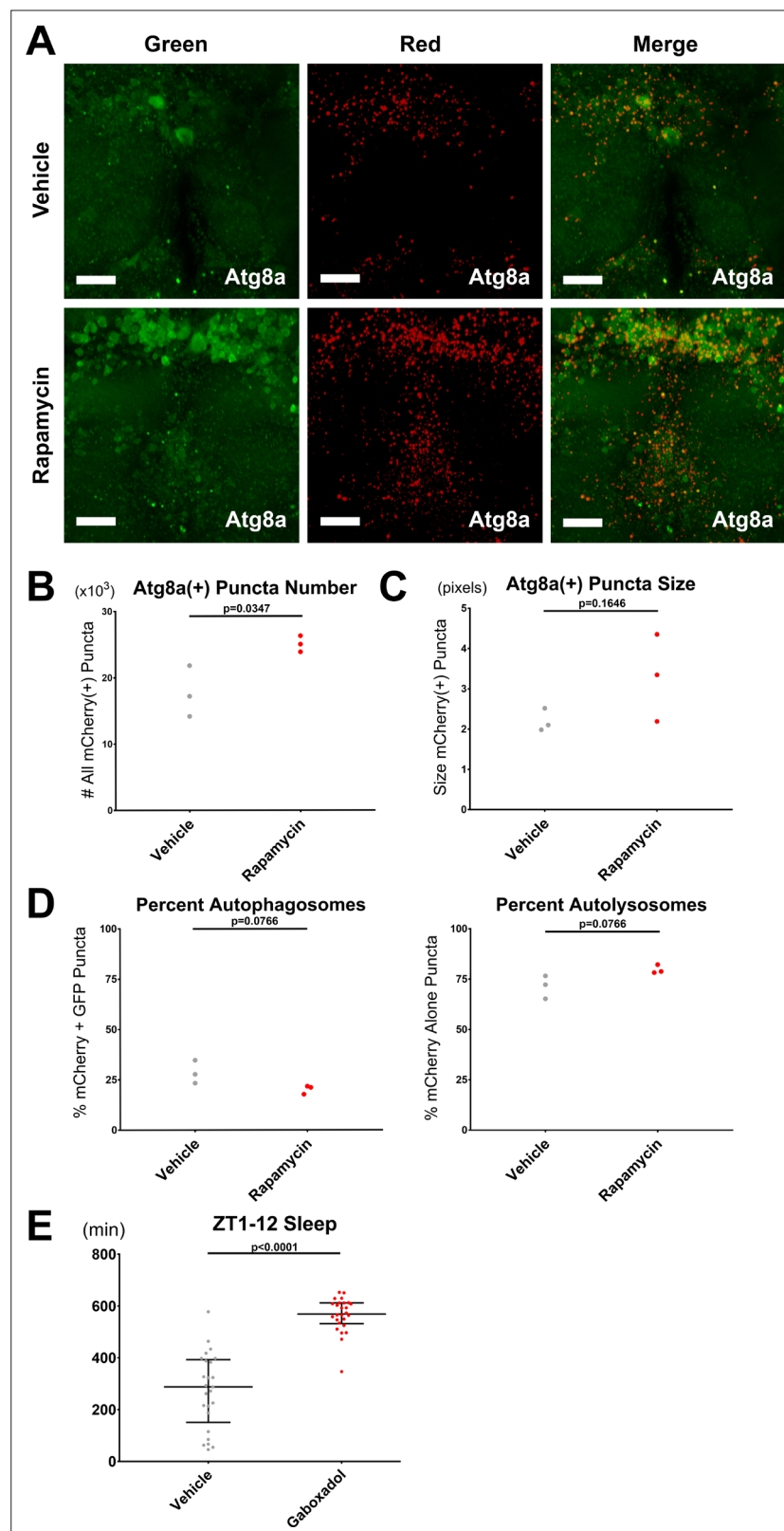


Figure 8—figure supplement 1. Validation of the Ilastik algorithm for scoring autophagy and the gaboxadol effect on sleep. (A–D) Female elav-Gal4> UAS-GFP-mCherry-Atg8a brains driving pan-neuronal autophagy sensor were live imaged from ZT2-4, after ~2 hr of pre-incubation in either vehicle or 2 μ M rapamycin supplemented AHL. mCherry fluoresces in all Atg8a(+) puncta, while GFP fluoresces in autophagosomes and is quenched in autolysosomes. (E) Sleep duration was measured in ZT1-12. *Figure 8—figure supplement 1 continued on next page*

Figure 8—figure supplement 1 continued

autolysosomes. *n* = 3; individual brains. **(A)** Max-projected z-stacks of representative brains showing GFP (left), mCherry (middle), and merged (right) fluorescence. Scale bar = 25 μ m. **(B)** The number of all neuronal mCherry(+) puncta was significantly increased by rapamycin treatment. **(C)** The size of all neuronal mCherry(+) puncta were similar in both groups. **(D)** The percentages of mCherry+ GFP(+) autophagosomes (left) and mCherry-only(+) autolysosomes (right) were similar in both groups. **(E)** Total sleep amount was measured in the same flies later dissected for live imaging in **Figure 8I–L**, from ZT1 (shortly after flip onto either vehicle or gaboxadol-laced food) to ZT12 (when the first fly live imaged was removed from the sleep monitors for dissection). As expected, gaboxadol feeding robustly increased sleep during this window. *n* = 25–26; individual flies overlaid with median \pm interquartiles; Student's t-test.

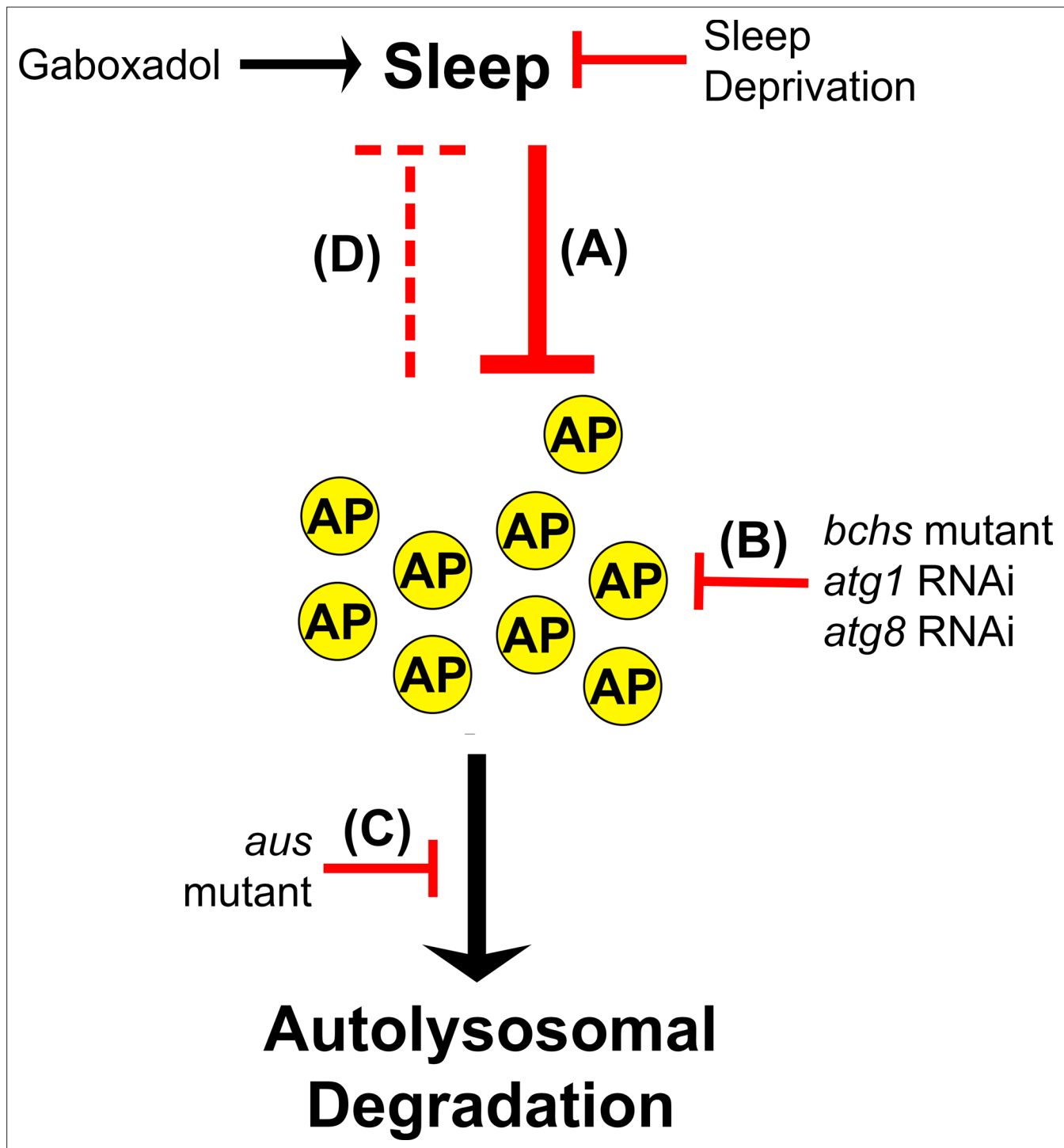


Figure 9. Model for sleep-autophagy interaction. This schematic details our model for how sleep and macroautophagy interact, based on our results. **(A)** Sleep decreases autophagosome number under normal conditions, in a manner that is sensitive to both gaboxadol gain or SD loss of sleep lasting between 11 and 14 hr. **(B)** The mutant *blue cheese*, pan-neuronal RNAi for *atg1*, and whole-fly RNAi for *atg8b* (suppressing both 8a and 8b homologs) are all known to inhibit autophagosome formation, and all increase sleep. **(C)** Neuronal loss-of-function in the *aus* mutant inhibits autophagosome degradation, and decreases sleep in a manner that is rescued by blocking autophagosome formation upstream. **(D)** The wake-promoting / sleep-inhibiting effects of autophagosome number are able to drive sleep behavior when strongly and sustainably adjusted by our genetic manipulations, but are unable to drive sustained waking after a single night of SD, as acute rebound sleep is well established to occur after sleep deprivation on this timescale. Together, this suggests that autophagosome inhibition of sleep is considerably weaker than sleep inhibition of autophagosome accumulation, with autophagosome number only becoming a strong enough signal to control sleep behavioral output with a very strong and/or sustained stimulus.